

High ^{222}Rn concentrations and dynamics in Shawan Cave, southwest China

Yanwei Wang^{a,b}, Weijun Luo^{b,c,*}, Guangneng Zeng^d, Yang Wang^b, Hanling Yang^{a,b},
Meifang Wang^{b,e}, Lin Zhang^{b,c}, Xianli Cai^{b,c}, Jia Chen^{b,c}, Anyun Cheng^{b,c}, Shijie Wang^{b,c}



^a University of Chinese Academy of Sciences, Beijing, 100049, China

^b State Key Laboratory of Environmental Geochemistry, Institute of Geochemistry, CAS, Guiyang, 550081, China

^c Puding Karst Ecosystem Research Station, CAS, Puding, 562100, China

^d School of Chemistry and Eco-Environmental Engineering, Guizhou Minzu University, Guiyang, 550025, China

^e School of Geography and Environmental Sciences, Guizhou Normal University, Guiyang, 550025, China

ARTICLE INFO

Keywords:

^{222}Rn
Cave ventilation
Dose exposure
Chimney effect
Karst

ABSTRACT

Cave ^{222}Rn has been a major health issue and subject of scientific debate for decades. While the basics of natural ventilation physics are well understood, it is difficult to make blind predictions of ^{222}Rn concentrations in a given cave due to the complexity of cave systems. In-situ continuous observation is necessary to improve our ability to quantify radiation dose exposure and reduce radiation hazard to cave users, and trace the air exchange patterns occurring in caves. In this study, continuous monitoring using a RAD7 radon detector revealed high ^{222}Rn concentrations and large fluctuations in ^{222}Rn concentration in a small karst cave in southwest China, Shawan Cave. From August 2016 to July 2017, the average annual concentration was $47,419 \text{ Bqm}^{-3}$ and ranged between 3720 and $123,000 \text{ Bqm}^{-3}$, with lower values during summer than other seasons. Taking Shawan Cave as a case study, we suggest a framework to evaluate the potential dose exposure, allowing cave users to minimize risk of exposure to hazardous levels of ^{222}Rn . Furthermore, we comparing results from this study with other studies in 35 caves worldwide, and conclude that there are three patterns of seasonal ^{222}Rn variation. They were classified into five types of ventilation mode based on diversity of cave locations, geometry and connectivity of bed rock fracture networks, together with temperature differences between outside atmosphere and cave air.

1. Introduction

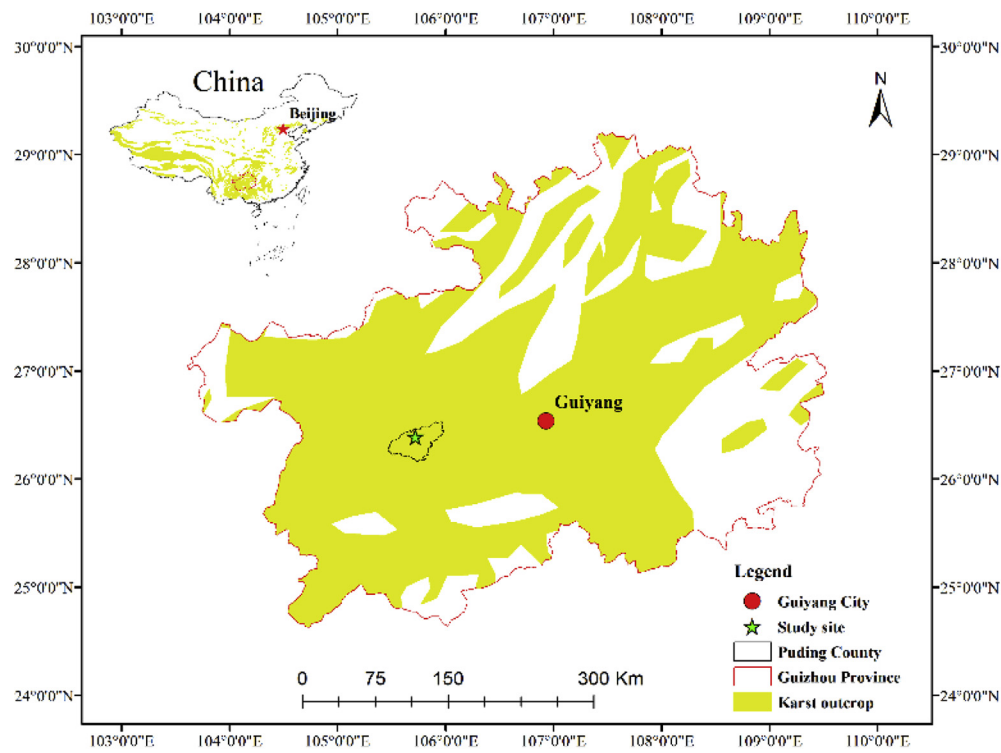
Radon is a radioactive gas originating as an intermediate product of ^{238}U (^{222}Rn), ^{235}U (^{219}Rn), and ^{232}Th (^{220}Rn) decay series. The most abundant radon isotope, ^{222}Rn (hereafter referred to as radon), is released from soils and rocks depending on both the concentration and the distribution of its parent nuclide, ^{226}Ra . Despite the very low uranium content in limestone, strong enrichment of uranium during weathering of carbonate rocks can occur, leading to a high uranium content in residual soils which are widespread throughout the fissures and karst cavities (Feng et al., 2013; H. R. Gunten et al., 1996; Tadolini and Spizzico, 1998). Combined with the enclosed space of cave systems, this leads to exceptionally high radon concentrations in karst caves worldwide (Cigna, 2005; Hakl et al., 1997; Hyland and Gunn, 1994; Tao et al., 2012).

Epidemiological studies have shown a clear link between breathing high concentrations of radon and incidence of lung cancer (Field, 2011; Robertson et al., 2013). It is hence necessary to categorize personal dosimetry in view of the potential health hazards caused by inhaling

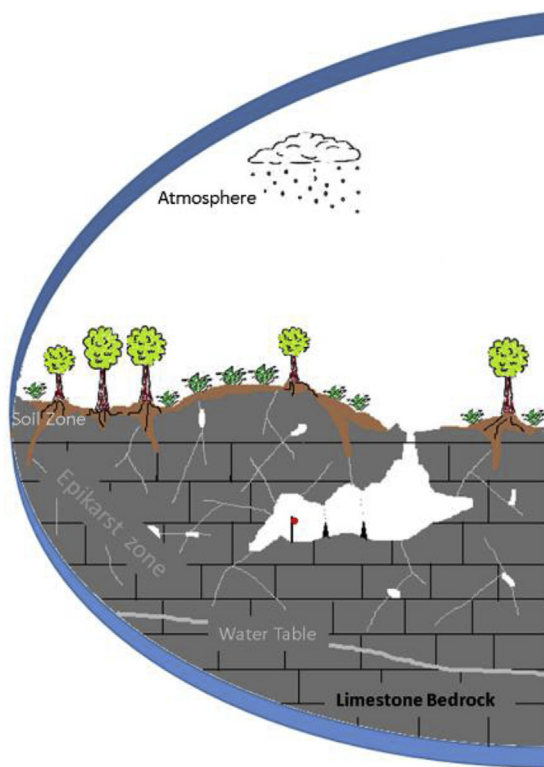
radon and its daughter nuclides in such environments. For example, a radon survey in seven caves in Romania found all exceeded the European Union reference level of radon gas in workplaces (300 Bqm^{-3}), meaning there is a potential health hazard to cave guides, cavers, and scientists (Cucoş et al., 2016). Additionally, radon as a noble gas is chemically inert and has a half-life of 3.8 days, which makes it highly useful as a natural tracer of underground airflow (Baskaran, 2016; Quindos Poncela et al., 2013), providing a non-invasive method for characterizing natural ventilation.

Karst landscapes are wide spread in China, covering an area of about 3400000 km^2 , and there are more than 500000 known caves in China, mostly located in the southwest karst region (Chen et al., 2006). Continuous radon monitoring in caves at an approximately hourly interval is necessary to perform the correct calculations of annual effective dose and elucidate details of ventilation processes (Lario et al., 2005). However, almost no continuous radon monitoring studies have been reported in the area (Shen, 1988; Tao et al., 2012; Yang et al., 2013). In this study, radon concentration was monitored for one year in a shallow karst cave (Shawan Cave) in Guizhou, Southwest China. Our

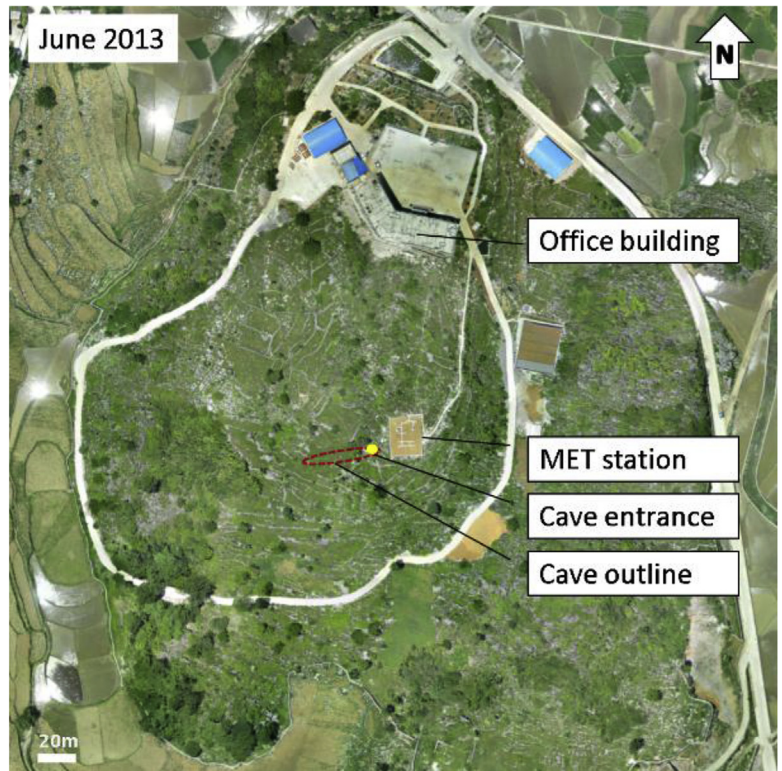
* Corresponding author. Institute of Geochemistry, Chinese Academy of Sciences, 99 Lincheng West Road, Guiyang, 550081, Guizhou Province, China.
E-mail address: luoweijun@vip.gyig.ac.cn (W. Luo).



(a)



(b)



(c)

Fig. 1. Location and geometry of the study cave. (a) Site location; (b) Schematic profile map of the study cave. The red point shows the location of the radon concentration, temperature, relative humidity and air pressure measurements; (c) Aerial view of the study area. (For interpretation of the references to colour in this figure legend, the reader is referred to the Web version of this article.)

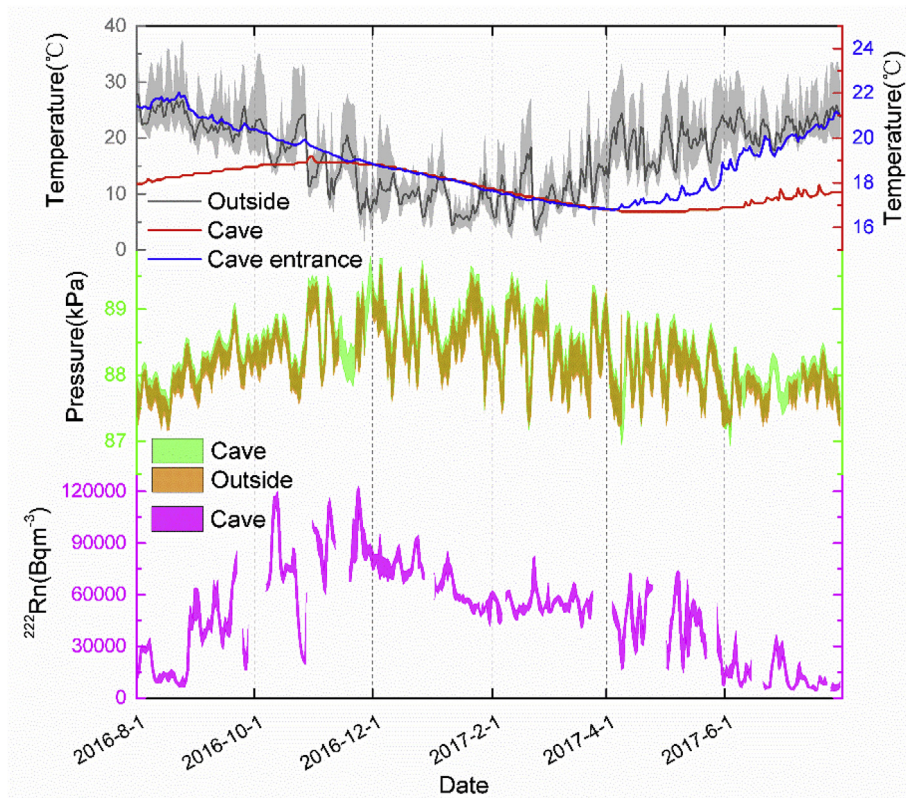


Fig. 2. Seasonal evolution of radon concentration and meteorological variables.

major goals are: to evaluate dose exposure risks for occasional cave users, to determine the environmental factors that affect radon concentration variation, and to improve understanding of the general exchange patterns of cave ventilation.

2. Materials and methods

2.1. Site description

The site (26.36°N, 105.76°E, 1170 m.a.s.l) is located in Puding County, Guizhou Province, which is at the center of the southwest karst region of China (Fig. 1a). This area belongs to the subtropical region of China and experiences a monsoonal climate. According to the Puding station meteorological station records, the mean annual air temperature of the region between 1961 and 2008 was 15.1 °C, and the annual average precipitation was 1367 mm, of which more than 70% occurs during the rainy season from April to September (Liu et al., 2016). The dominant lithology is the pure and thick Guanling Formation limestone of the Middle Triassic (T₂). The black limestone soil (Rendzina, in FAO and China's soil taxonomy classifications) is shallow (20–50 cm), discontinuous, and highly heterogeneous. The vegetation is mainly tree-shrub-grassland mosaic (Fig. 1c). The study cave is at the top of a small hill, the accessible passage of the cave is about 10 m deep and 30 m long, and the only identified opening is above the cave passage at one end with an area of less than 1 m² (Fig. 1b). The passage is irregular, about 3 m wide and 3 m high, and contains speleothems such as stalagmites, soda straws and draperies.

2.2. Radon detection method

In situ radon gas was measured using a RAD7 Radon Detector (Durrigge Company Inc., USA). The RAD7 measures radon gas concentration using a solid state alpha detector, by measuring the alpha spectrometry of the decay products (Almayahi et al., 2013). The

detector was calibrated by Durrigge Company with a calibration accuracy of $\pm 5\%$. The working range is from approximately 4 Bqm⁻³ to 750000 Bqm⁻³, the operating temperature range is from 0 to 45 °C, and the operating humidity range is from 0 to 100%. RAD7 was configured to NORMAL mode with user specification, which allowed continuous half-hourly measurements of radon gas concentration. This mode was used to record the long term dynamics of radon concentration. The built-in pump typically draws cave air at a flow rate of 800 mL/min. The desiccant in the humidity measurement chamber was replaced every two weeks to reduce the chamber humidity to below 10%; when humidity exceeds the limit, an automatic correction is applied. The cave entrance temperature and relative humidity were measured with a HOBO Pro V2 data logger (ONSET Company Inc., USA). Temperature accuracy is ± 0.21 , relative humidity accuracy is $\pm 2.5\%$ for 10% RH to 90% RH, $\pm 5\%$ for above 90% RH and below 10% RH, and the cave air pressure and temperature with a HOBO U20L-04 logger (ONSET Company Inc., USA). Pressure accuracy is 0.1%, temperature accuracy is ± 0.37 °C; both recorded measurements every half-hour and were placed 1 m above floor height inside the cave. The outside air temperature and pressure were measured by an automatic meteorological station.

Currently, the International Commission on Radiological Protection (ICRP) uses the dose conversion convention to calculate effective dose per unit exposure to radon and its progeny. Based on the recommendations of latest publication of ICRP (Paquet et al., 2017), we use the dose conversion factor of approximately 20 mSvWLM⁻¹ which is recommended for workers in tourist caves. And to calculate the WLM by formula:

$$\text{WLM} = \frac{\sum (C_{Rn} Ft)}{3700 \text{Bqm}^{-3} \times 170h}$$

Where C_{Rn} is the radon level measured in the cave, F is the equilibrium factor and t is time spent in the cave, the equilibrium factor used was 0.4.

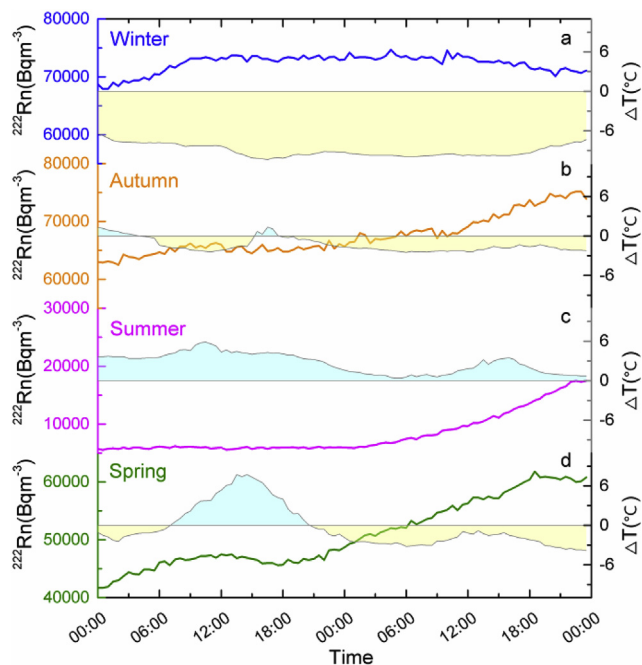


Fig. 3. Half hourly change of cave radon concentration and environmental variables. ΔT refers to the temperature difference (outside atmosphere temperature minus cave air temperature). (a) Dec 19 to 20, 2016 during the winter period; (b) Oct 8 to 9, 2016 during the autumn period; (c) Jun 24 to 25, 2016 during the summer period; (d) May 5 to 6, 2017 during the spring period.

3. Results and discussion

3.1. Trends of radon concentration and meteorological variables in Shawan cave

During the study period, the average daily temperature in Shawan cave was 17.8 °C with a range of approximately 2 °C, while the average daily outside air temperature was 16.7 °C with a range of 35 °C, and the maximum cave temperature lagged about three months behind peak of outside air temperature (Fig. 2). Limestone is an insulator with a low coefficient of heat conductivity (Stoeva et al., 2006), therefore the conductive heat flux due to outside annual thermal oscillations cannot induce significant temperature variations at depths greater than 5 m (Luetscher and Jeannin, 2004). The 2 °C temperature range variation inside the cave should hence be induced primarily by heat fluxes related

to water and/or air circulations. The descending temperature inside the cave during late autumn to early spring is probably due to exchange of cave air with outside cold atmospheric air, while the rising temperature during late spring to early autumn is probably due to exchange with warm atmospheric air. The temperature at the cave entrance changes synchronously with the inside cave temperature during the cold dry season as the result of cave air rising, which is a frequently observed phenomenon. On the contrary, the temperature at the cave entrance follows closely behind the outside atmospheric air temperature during the warm, rainy season, which indicates that the direction of air movement is downward into the cave (Fig. 2). Air pressure in the cave fluctuates synchronously with outside air pressure and both show an opposing trend to atmospheric temperature change (Fig. 2). The simultaneous variations of air pressure in the cave and outside the cave show that the cave is a well-ventilated system (Šebela and Turk, 2011).

The annual average radon concentration during the study period was 49335 Bqm⁻³, and ranged between 3720 and 123000 Bqm⁻³. Lower values are observed in summer and higher values in winter, with significant variability during autumn and spring (Fig. 2). The radon concentration observed in this study is much higher than previous cave radon studies in China and is among the highest of the reported studies all over the world (Fig. 7). For example, a study of 11 caves distributed across China found radon concentrations ranging between 263 and 4658.4 Bqm⁻³ (Wei, 1998), while a study of 11 karstic caves open to tourists in Guizhou Province found radon concentrations ranging between 11.5 and 5076 Bqm⁻³ (Shen, 1988). A study in 10 limestone tunnels built in mountain ranges found radon concentrations ranging from 38 to 570 Bqm⁻³ (Li et al., 2010), and the world annual average radon concentration taken from measurements in 220 different caves is 2800 Bqm⁻³, ranging between 100 and 20000 Bqm⁻³ (Hakl et al., 1997).

The pattern of radon concentration variation in the study cave is contrary to general observed patterns of high summer values and low winter values, such as observed in studies in Xueyu Cave (Yang et al., 2013), Postojna Cave (Gregorič et al., 2011) and Hollow Ridge Cave (Kowalczk and Froelich, 2010), but is in accordance with studies in Altamira Cave (Sainz et al., 2018), Candamo Cave (Hoyos et al., 1998) and Castañar Cave (Lario et al., 2006). During the winter period, the difference between outside air and cave air temperature is typically negative (cave temperature is higher), and radon concentration is relatively high and correlates with temperature difference, i.e. higher values are observed when temperature differences were getting larger (Fig. 3a). On the contrary, the temperature difference was typically positive during the summer period, radon concentration is relatively low, and generally higher values are observed when temperature

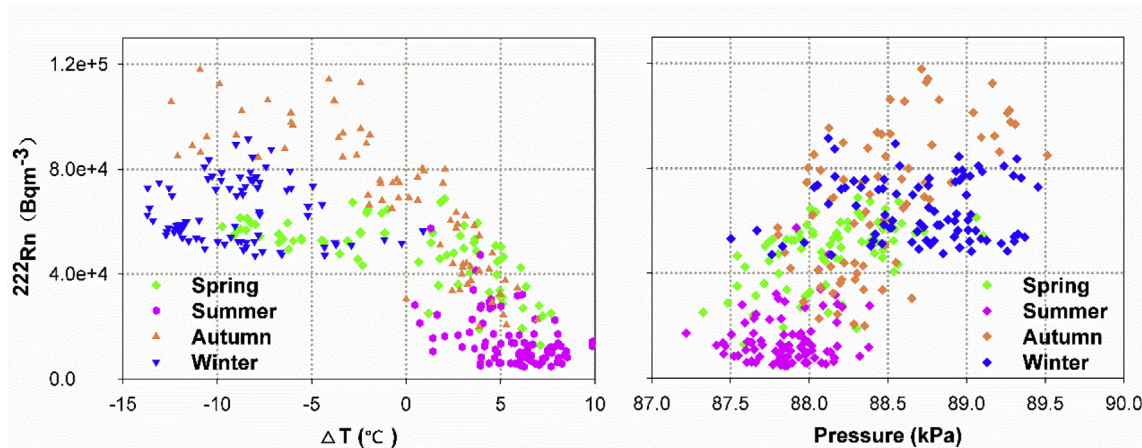


Fig. 4. Relation between cave radon concentration and environmental variables. ΔT refers to the temperature difference between outside atmospheric air and cave air. (a) Relationship between cave radon concentration and the temperature difference, the linear correlation coefficients is -0.78 ($p = 0.01$); (b) Relationship between cave radon concentration and cave air pressure, the linear correlation coefficients is 0.68 ($p = 0.01$).

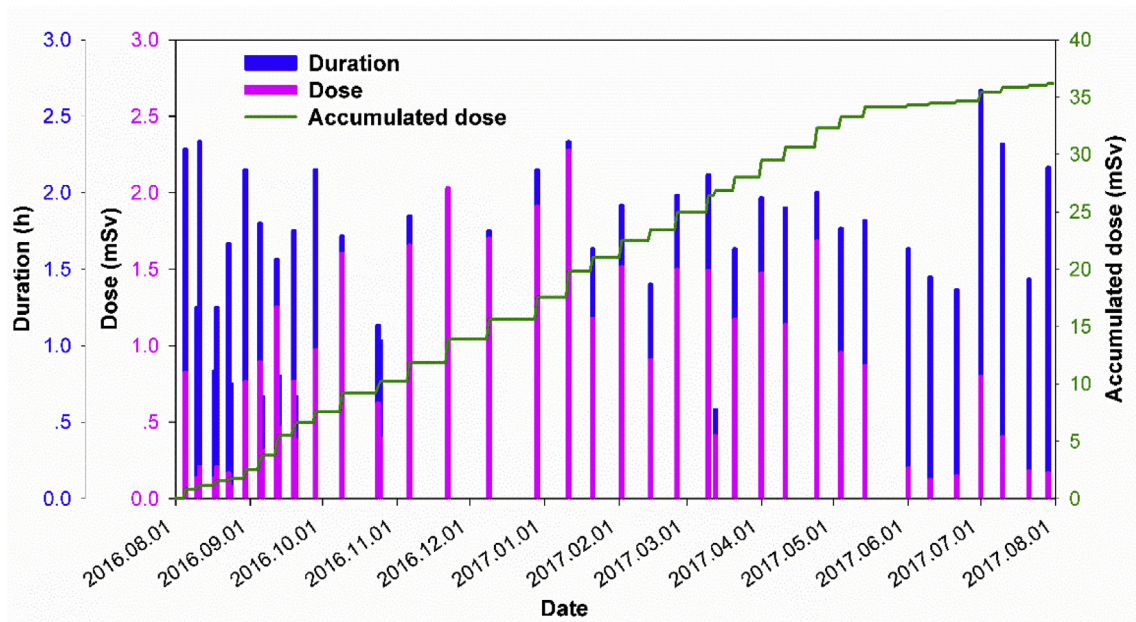


Fig. 5. Duration and personal dose exposure for cave user.

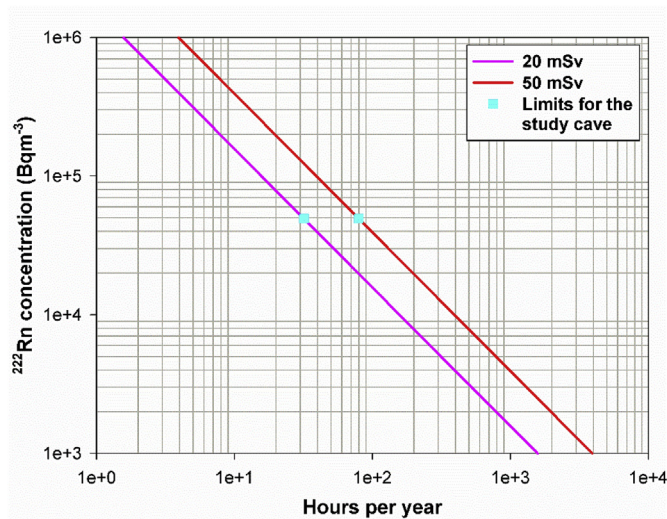


Fig. 6. Time limit of different reference levels for average radon concentration in Shawan Cave.

differences was getting small (Fig. 3c). The temperature difference is generally small but changes frequently during autumn and spring, radon concentration is relatively high, and higher values are observed when the temperature difference was getting negative (Fig. 3b,d).

Generally, temperature difference and cave radon concentration shows a negative relationship, while cave air pressure and radon concentration shows a positive relationship. This may indicate the existence of undiscovered connectivity below the cave passage, resulting in cave ventilation being dominated by the chimney effect (Fig. 4). The fissured nature of limestone lithology provides migration pathways for radon, resulting in the size of the underground ventilation system being much larger than the cave volume itself. The results may be reasonably explained by the interaction of cave ventilation with a reservoir of radon enriched air held within the small voids of the bed rock and soil profile as well as with the outside atmospheric air. In summer, the cave air as well as air stored in fissures is much colder than the outside atmospheric air and probably moves downward, resulting in atmospheric air being sucked into the cave through the upper opening and mixing

with the cave air. This would explain the low radon concentration observed in the upper cave chamber during summer. On the contrary, cave air and fissured air is much warmer than the outside atmospheric air and probably moves upward during winter, causing migration of the radon rich gas in the fissured space to the upper cave chamber, which would result in the high observed radon concentration in winter. In spring and autumn, the temperature difference between atmospheric air and cave air is generally small, which will result in minimal ventilation, causing radon accumulation in the cave chamber and the high observed concentrations. Additionally, frequent changes in weather systems lead to rapid and large air temperature changes which would explain the sharp fluctuations of radon concentration observed in the cave.

3.2. Evaluation of dose exposure in Shawan Cave

The significant monthly fluctuations in radon concentration indicate that the annual average radon concentration as well as the exact dose exposure in the study cave can only be accurately obtained by year-long measurements. As exact time recorded, the annual dose exposure calculated for a scientist who spent totally 69.6 h in the cave is up to 36.18 mSv (Fig. 5). This is about 15 times higher than the natural background radiation dose which is assumed 2.4 mSv per year (Hendry et al., 2009). This is also higher than the recommend limit of 20 mSv by ICRP (Vennart, 1991). The result suggest that a reduction or optimization of time spent inside the cave should be advised.

At levels above 100000 Bqm^{-3} even very short exposures lead to a high dose. The study cave appears as a high radiation environment with an annual total radiation dose of about 5489 mSv (Table .1). As there is not yet a scientifically established dose threshold for radiation hazard, the recommendations by the ICRP are adopted. The dose limit recommended by the ICRP for effective dose is 20 mSv per year averaged over a period of 5 years, with the condition that the effective dose should not exceed 50 mSv in any single year (Vennart, 1991). As the modification of the natural microclimate of caves should be avoided, the only way to reduce radon exposure is to apply a restriction in terms of time spent in the cave. For the study cave, with the average radon concentration being up to 49335 Bqm^{-3} , a time limit of 31.9 h per year with an equal monthly time distribution is recommended, and not in exceedance of 79.7 h for any single year (Fig. 6). Due to the radon concentration variation in the cave, with an equal monthly dose

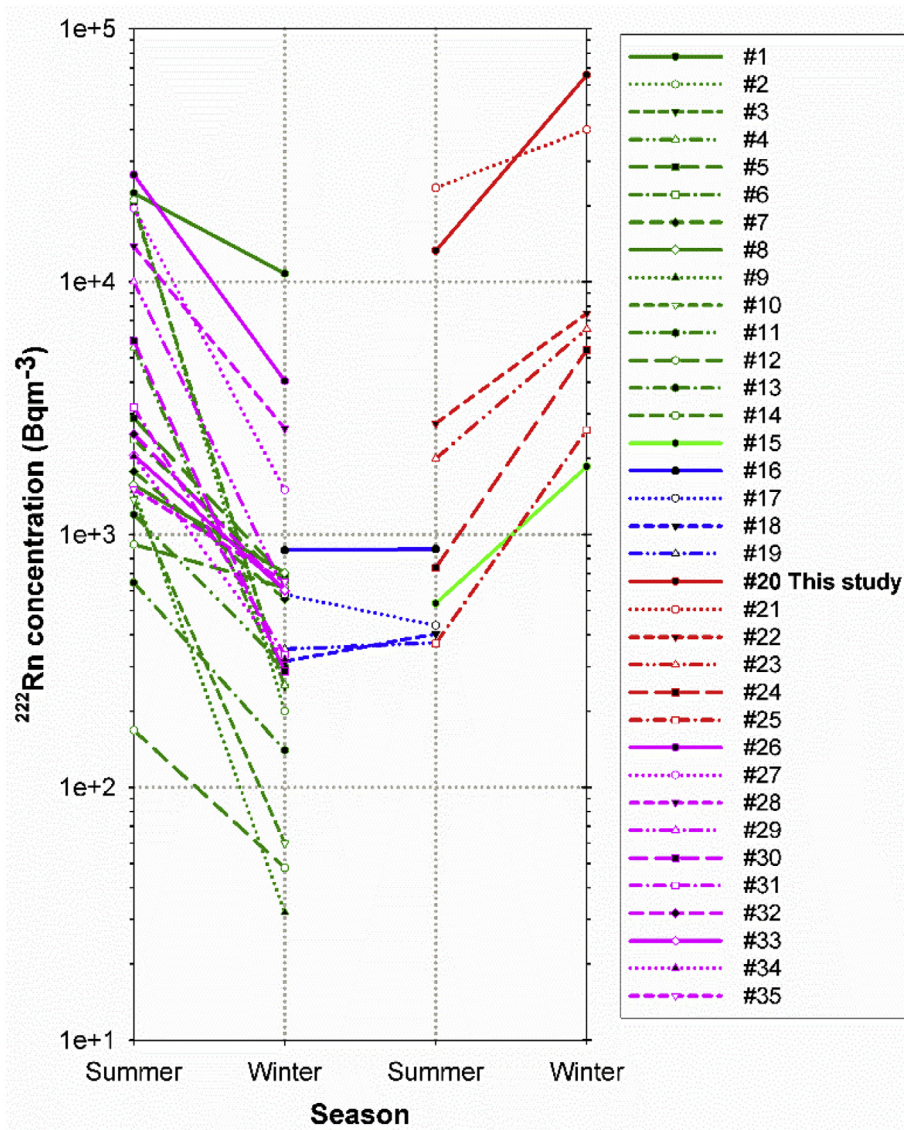


Fig. 7. Comparison of seasonal patterns of radon concentration variation for 35 caves worldwide. #1 refers Petralona Cave; #2 refers Kispaplika Cave; #3 refers Causse d’Aumelas Cave; #4 refers Pál-völgy Cave; #5 refers Rull Cave; #6 refers Tausoare Cave; #7 refers Carlsbad Cave; #8 refers Lantian Cave; #9 refers Gyokusenu-do Cave; #10 refers Radoochowska Cave; #11 refers Aven Cave; #12 refers Scărișoara Cave; #13 refers Seongru Cave; #14 refers Nerja Cave; #15 refers Muierii Cave; #16 refers Vadu Crisului Cave; #17 refers Tianxing Cave; #18 refers Despicătura Cave; #19 refers Xiniu Cave; #20 refers Shawan Cave; #21 refers Castañar Cave; #22 refers Pietró Cave; #23 refers Tüskés Cave; #24 refers Altamira Cave; #25 refers Candamo Cave; #26 refers Aktív Cave; #27 refers Sózó Cave; #28 refers Hollow Ridge Cave; #29 refers Abaliget Cave; #30 refers Xueyu Cave; #31 refers Creswell Cave; #32 refers Postojna Cave; #33 refers Vântului Cave; #34 refers Niedźwiedzia Cave; #35 refers Urșilor Cave.

Table 1
Summary of monthly average radon concentration and dose exposure.

Month	Radon concentration (Bqm ⁻³)	Dose/Month (mSv)	Dose/2.65 h (mSv)	Hours/1.66 mSv (hours)
Aug-16	19267	113.77	0.65	6.77
Sep-16	45844	261.97	1.55	2.85
Oct-16	70871	418.78	2.39	1.84
Nov-16	91878	525.02	3.10	1.42
Dec-16	77225	455.99	2.60	1.69
Jan-17	60758	358.76	2.05	2.15
Feb-17	55792	297.56	1.88	2.34
Mar-17	54719	323.10	1.84	2.39
Apr-17	47704	272.60	1.61	2.74
May-17	41793	246.78	1.41	3.12
Jun-17	16549	94.57	0.56	7.89
Jul-17	9625	56.83	0.32	13.56
Average(Total)	49335	457.48(5489.73)	1.66(19.95)	4.06(48.75)

distribution, a total time of 48.75 h can be spent without exceeding the limit of 20 mSv (Table .1). This dose exposure evaluation hence provides cave users with a framework to exercise judgement on when and how long they can visit the cave, to limit their dose exposure to safe limits while meeting their work requirements.

3.3. Comparison and classification of ventilation regime

Radon is a convenient natural tracer of air exchange between caves and atmosphere in karstic systems. As changes in radon production from within caves are expected to be small, the ventilation process is the main factor controlling changes of radon concentration in cave air (Przylibski, 1999). Positive increments in radon concentration inside a

Table 2
Classification of cave ventilation types.

Cave type (simplified)	Complexity	Ventilation mode	Seasonal radon pattern		Reference
			Summer	Winter	
	Simple	I Cold trap	High	Low	1 (Papastefanou et al., 2003); 2 (G Koltai, 2014); 3 (Batiot-Guilhe et al., 2007); 4 (Nagy et al., 2012); 5 (Pla et al., 2016); 6,12 (Cucos̆ et al., 2016); 7 (Wilkening and Watkins, 1976); 8 (Lu et al., 2009); 9 (Tanahara et al., 2008); 10 (Przylibski, 1999); 11 (Bourges et al., 2006); 13 (Hwa Oh and Kim, 2015); 14 (Dueñas et al., 1999)
		II Heat trap	Low	High	15 (Cucos̆ et al., 2016)
		III No trap	Low	Low	16 (Cucos̆ et al., 2016); 17 (Shen, 1988); 18 (Cucos̆ et al., 2016); 19 (Shen, 1988)
	Complex	IV Chimney effect	Low	High	20 (This study); 21 (Fernandez-Cortes et al., 2011); 22,23 (Koltai et al., 2010); 24 (Sainz et al., 2018); 25 (Hoyos et al., 1998)
		V Chimney effect	High	Low	26,27 (Koltai et al., 2010); 28 (Kowalczk and Froelich, 2010); 29 (G Koltai, 2014); 30 (Yang et al., 2013);

(continued on next page)

Table 2 (continued)

Cave type (simplified)	Complexity	Ventilation mode	Seasonal radon pattern		Reference
			Summer	Winter	
					31 (Gillmore et al., 2002);
					32 (Gregorič et al., 2011);
					33,34 (Cucuş et al., 2016);
					35 (Przylibski, 1999);

cave can only be due to its increased isolation with respect to the outside atmosphere, or to a supply of air from adjacent fissured space containing significantly higher concentrations of the gas. Likewise, reductions in radon concentration in caves can only be produced by radioactive decay or due to an air supply containing a lower concentration of the gas, usually from more superficial or external locations (Sainz et al., 2018). Here, 35 caves from reported studies worldwide are summarized and show 3 different patterns of seasonal radon variation (Fig. 7). The first pattern shows high summer and low winter radon concentration, the second pattern shows low and comparable radon concentration for both seasons, and the third pattern shows high winter and low summer concentrations. Combined with detailed cave characteristics, they are further classified into 5 types of ventilation mode (Table 2).

For type I, caves with only an upper opening and minimal fissure development below the cave floor act as a cold trap. Ventilation develops in the winter because the cave temperature is higher than the outside air temperature, convection induced air exchange allowing the warmer cave air to rise to the entrance and the colder outside air to enter the cave, which results in a low radon concentration in the cave. The reverse occurs in summer, when the outside air temperature is much higher than inside the cave and keeps the cave air stagnant, causing radon gas to accumulate to high concentrations. Examples of this ventilation mode include Lantian Cave in China (Lu et al., 2009), L'Aven D'Orgnac Cave in France (Bourges et al., 2006), and Nerja Cave in Spain (Dueñas et al., 1999). Type II caves are characterized by an opening at the base of the cave and minimal fissure development above the cave roof, resulting in the cave acting as a heat trap. The air mass would be stable in winter with hot air remaining trapped in the cavity, while in summer it would be ventilated when cavity air flows out due to its density being higher than the outside air density. Type II caves are hence characterized by a high radon concentration in winter and a low radon concentration in summer, an example being Muierii Cave in Romania (Cucuş et al., 2016). Type III caves are characterized by a relatively horizontal shape, an opening at one end, and minimal fissure development, resulting in bidirectional convective air flow throughout the year and consequently a generally low radon concentration compared with other cave types. Examples include Xiniu Cave and Tianxing Cave in Zhenning (Shen, 1988), and Vadu crislui Cave and Despica-tura Cave in Romania (Cucuş et al., 2016). Type IV caves are situated near the ground surface with an extensive below-cave fissure network, resulting in the chimney effect dominating the ventilation process. High winter radon concentrations are driven by upward cave airflow that brings radon accumulated in the fractures of the rock matrix into the cave chamber, while low summer concentrations are caused by suction of atmospheric air into the cave from the surface, diluting the radon concentration in the chamber near the entrance. Examples include Shawan Cave (this study), Candamo Cave, Altamira Cave and Castañar Cave in Spain (Hoyos et al., 1998), and Pietró Cave and Tüskés Cave in

Hungary (Koltai et al., 2010). Type V caves are situated in lower topographical positions, have an extensive above-cave fissure network, and the chimney effect also dominates the ventilation process, but the seasonal radon concentration variation is reversed. Examples include Xueyu cave in China (Yang et al., 2013), Postojna cave in Slovenia (Gregorič et al., 2011), and Hollow ridge cave in USA (Kowalczk and Froelich, 2010).

Each of these cave systems may have an element of uniqueness but all follow the general principles of one of the five ventilation models described above. Karstic strata is characterized by a series of interconnected larger openings and fractures due to the chemical dissolution in the rock matrix by infiltrating waters, so a volume much larger than the principle cave cavity is often involved in the control of the internal cave atmosphere. A better understanding of ventilation patterns has important practical applications for cave users to optimize time spend in the cave and reduce potential radon hazard.

4. Conclusion

The increased radiation exposure to users of karst caves with elevated radon concentrations poses a potentially significant health hazard. It is of great importance both for cave protection and visitor's health to identify the period of greatest ventilation when hazardous gas concentrations are at a minimum. This study can assist in developing guidelines to advise cavers on best practice to minimize radon exposure in caves. Additionally, the suggested models of seasonal radon concentration changes in caves provide evidence of the uniqueness of air exchange patterns in cave systems and also of the complex nature of cave ventilation, which is critical to trace and interpret vadose zone processes.

Acknowledgements

This study was supported jointly by National Key Research and Development Program of China (2016YFC0502300, 2016YFC0502102), the National Natural Science Foundation of China (41571130042, 41673121, 41571130074 and 41663015), and Foundation of Guizhou educational committee KY [2016] 159. We also thank anonymous reviewers for their valuable comments and suggestions on this manuscript, and we thank Sarah Buckerfield for language improvement.

References

- Almayahi, B.A., Tajuddin, A.A., Jaafar, M.S., 2013. In situ soil ^{222}Rn and ^{220}Rn and their relationship with meteorological parameters in tropical Northern Peninsular Malaysia. *Radiat. Phys. Chem.* 90, 11–20.
- Baskaran, M., 2016. *Radon: a Tracer for Geological, Geophysical and Geochemical Studies*. Springer International Publishing.
- Batiot-Guilhe, C., Seidel, J.-L., Jourde, H., Hébrard, O., Bailly-Comte, V., 2007. Seasonal

- variations of CO₂ and ²²²Rn in a mediterranean sinkhole - spring (Causse d'Aumelas, SE France). *Int. J. Speleol.* 36 (1), 51–56.
- Bourges, F., Genthon, P., Mangin, A., D'Hulst, D., 2006. Microclimates of l'Aven d'Orgnac and other French limestone caves (Chauvet, Esparros, Marsoulas). *Int. J. Climatol.* 26 (12), 1651–1670.
- Chen, W., Beijing, Guilin, 2006. An outline of speleology research progress. *Geol. Rev.* 52 (6), 783–792.
- Cigna, A.A., 2005. Radon in caves. *Int. J. Speleol.* 34 (1–2), 1–18.
- Cucoş, A.D., et al., 2016. Radon levels in Romanian caves: an occupational exposure survey. *Environ. Geochem. Health* 39 (5), 1–15.
- Dueñas, C., Fernández, M.C., Cañete, S., Carretero, J., Liger, E., 1999. ²²²Rn concentrations, natural flow rate and the radiation exposure levels in the Nerja Cave. *Atmos. Environ.* 33 (3), 501–510.
- Feng, Z.G., Ma, Q., Wang, S.J., Li, S.P., Liang, L.D., 2013. The enrichment characteristics of uranium and thorium in weathering profiles of carbonate rocks and the implications of their leaching experiments. *Geol. Bull. China* 32 (4), 639–651.
- Fernandez-Cortes, A., Sanchez-Moral, S., Cuezva, S., Benavente, D., Abella, R., 2011. Characterization of trace gases' fluctuations on a 'low energy' cave (Castañar de Ibor, Spain) using techniques of entropy of curves. *Int. J. Climatol.* 31 (1), 127–143.
- Field, M.S., 2011. Risks to cavers and cave workers from exposures to low-level ionizing α radiation from ²²²Rn decay in caves. *J. Cave Karst Stud. Natl. Speleol. Soc. Bull.* 69 (1), 207–228.
- Koltal, G., T, Z., H, E., 2014. First results of the radon concentration monitoring in Abaliget and Kispaplika caves. *Acta Climatol. Chorol.* 47–48, 71–76 Tomus.
- Gillmore, G.K., Phillips, P.S., Denman, A.R., Gilbertson, D.D., 2002. Radon in the creswell crags Permian limestone caves. *J. Environ. Radioact.* 62 (2), 165–179.
- Gregorič, A., Zidanšek, A., Vaupotič, J., 2011. Dependence of radon levels in Postojna Cave on outside air temperature. *Nat. Hazards Earth Syst. Sci.* 11 (5), 1523–1528.
- Gunten, H.R.V., Surbeck, H., Rössler, E., 1996. Uranium series disequilibrium and high thorium and radium enrichments in karst formations. *Environ. Sci. Technol.* 30 (4), 1268–1274.
- Hakl, J., et al., 1997. Radon transport phenomena studied in Karst caves-international experiences on radon levels and exposures. *Radiat. Meas.* 28 (1), 675–684.
- Hendry, J.H., et al., 2009. Human exposure to high natural background radiation: what can it teach us about radiation risks? *J. Radiol. Prot.* 29 (2A), A29–A42.
- Hoyos, M., Soler, V., Cañaveras, J.C., Sánchezmoral, S., Sanzrubio, E., 1998. Microclimatic characterization of a karstic cave: human impact on microenvironmental parameters of a prehistoric rock art cave (Candamo Cave, northern Spain). *Environ. Geol.* 33 (4), 231–242.
- Hwa Oh, Y., Kim, G., 2015. A radon-thoron isotope pair as a reliable earthquake precursor. *Sci. Rep.* 5, 13084.
- Hyland, R., Gunn, J., 1994. International comparison of cave radon concentrations identifying the potential alpha radiation risks to British cave users. *Health Phys.* 67 (2), 176–179.
- Koltai, G., Orszag, J., Tegzes, Z., Barany-Kevei, I., 2010. Comprehensive radon concentration measurements in caves located in the area of Mecsek mountains. *Acta Carsol.* 39 (3), 513–533.
- Kowalczyk, A.J., Froelich, P.N., 2010. Cave air ventilation and CO₂ outgassing by radon-²²² modeling: how fast do caves breathe? *Earth Planet. Sci. Lett.* 289 (1–2), 209–219.
- Lario, J., Sanchez-Moral, S., Canaveras, J.C., Cuezva, S., Soler, V., 2005. Radon continuous monitoring in Altamira Cave (northern Spain) to assess user's annual effective dose. *J. Environ. Radioact.* 80 (2), 161–174.
- Lario, J., Sanchezmoral, S., Cuezva, S., Taborda, M., Soler, V., 2006. High ²²²Rn levels in a show cave (Castañar de Ibor, Spain): proposal and application of management measures to minimize the effects on guides and visitors. *Atmos. Environ.* 40 (38), 7395–7400.
- Li, X., Song, B., Zheng, B., Wang, Y., Wang, X., 2010. The distribution of radon in tunnels with different geological characteristics in China. *J. Environ. Radioact.* 101 (5), 345–348.
- Liu, L., et al., 2016. Biomass of karst evergreen and deciduous broad-leaved mixed forest in central Guizhou province, southwestern China: a comprehensive inventory of a 2 ha plot. *Silva Fenn.* 50 (3), 16.
- Lu, X., Li, L.Y., Zhang, X., 2009. An environmental risk assessment of radon in Lantian Karst Cave of Shaanxi, China. *Water, Air, Soil Pollut.* 198 (1–4), 307–316.
- Luetscher, M., Jeannin, P.Y., 2004. Temperature distribution in karst systems: the role of air and water fluxes. *Speleogenesis & Evol. Karst Aquif.* 16 (6), 344–350.
- Nagy, H.E., et al., 2012. Time variations of ²²²Rn concentration and air exchange rates in a Hungarian cave. *Isot. Environ. Health Stud.* 48 (3), 464–472.
- Papastefanou, C., Manolopoulou, M., Stoulos, S., Ioannidou, A., Gerasopoulos, E., 2003. Radon concentrations and absorbed dose measurements in a Pleistocene cave. *J. Radioanal. Nucl. Chem.* 258 (1), 205–208.
- Paquet, F., et al., 2017. ICRP publication 137: occupational intakes of radionuclides: Part 3. *Ann. ICRP* 46 (3–4), 1–486.
- Pla, C., et al., 2016. Changes in the CO₂ dynamics in near-surface cavities under a future warming scenario: factors and evidence from the field and experimental findings. *Sci. Total Environ.* 565, 1151–1164.
- Przylibski, T.A., 1999. Radon concentration changes in the air of two caves in Poland. *J. Environ. Radioact.* 45 (1), 81–94.
- Quindos Poncela, L., Sainz Fernandez, C., Fuente Merino, I., Gutierrez Villanueva, J., Gonzalez Diez, A., 2013. The use of radon as tracer in environmental sciences. *Acta Geophys.* 61 (4), 848–858.
- Robertson, A., Allen, J., Laney, R., Curnow, A., 2013. The cellular and molecular carcinogenic effects of radon exposure: a review. *Int. J. Mol. Sci.* 14 (7), 14024–14063.
- Sainz, C., et al., 2018. Continuous monitoring of radon gas as a tool to understand air dynamics in the cave of Altamira (Cantabria, Spain). *Sci. Total Environ.* 624, 416–423.
- Šebela, S., Turk, J., 2011. Local characteristics of Postojna Cave climate, air temperature, and pressure monitoring. *Theor. Appl. Climatol.* 105 (3–4), 371–386.
- Shen, G., 1988. Radon concentration in scenic karstic caves in Guizhou Province. *J. Guizhou Univ.* 5 (4), 295–299.
- Stoeva, P., Stoev, A., Kiskinova, N., 2006. Long-term changes in the cave atmosphere air temperature as a result of periodic heliophysical processes. *Phys. Chem. Earth, Parts A/B/C* 31 (1–3), 123–128.
- Tadolini, T., Spizzico, M., 1998. Relation between "terra rossa" from the Apulia aquifer of Italy and the radon content of groundwater: experimental results and their applicability to radon occurrence in the aquifer. *Hydrogeol. J.* 6 (3), 450–454.
- Tanahara, A., Taira, H., Takemura, M., 2008. Radon distribution and the ventilation of a limestone cave on Okinawa. *Geochem. J. GJ* 31 (1), 49–56.
- Tao, Z.I., Yang, X.X., Shi, D.F., 2012. Review of the research on radon in karst caves. *Carsol. Sin./Zhong Guo Yan Rong* 31 (1), 99–106.
- Vennart, J., 1991. The 1990 recommendations of the international Commission on radiological protection. *J. Radiol. Prot.* 11 (3), 199–203.
- Wei, L., 1998. Source, distribution and determination of cave radon. *Carsol. Sin./Zhong Guo Yan Rong* 17 (3), 251–253.
- Wilkening, M.H., Watkins, D.E., 1976. Air exchange and ²²²Rn concentrations in the Carlsbad Caverns. *Health Phys.* 31 (2), 139–145.
- Yang, X.X., Tao, Z.I., Chen, B.Q., Xiang, X., Wang, X.X., 2013. Variation characteristics of the radon's concentration and protection to the harm in the Xueyu cave, Chongqing. *Carsol. Sin./Zhong Guo Yan Rong* 32 (4), 472–479.